PHILOSOPHICAL TRANSACTIONS OF THE ROYAL SOCIETY A
MATHEMATICAL, PHYSICAL & ENGINEERING SCIENCES

Experiments on a two–dimensional laminar separation bubble

C. P. Häggmark, A. A. Bakchinov and P. H. Alfredsson

Phil. Trans. R. Soc. Lond. A 2000 **358**, 3193-3205
doi: 10.1098/rsta.2000.0704

10.1098/rsta.2000.0704

Experiments on a two-dimensional laminar separation bubble

By C. P. Häggmark†, A. A. Bakchinov‡ and P. H. Alfredsson
Department of Mechanics, KTH, S-100 44 Stockholm, Sweden

A two-dimensional separation bubble on a flat plate is studied experimentally by means of hot-wire anemometry and flow visualization. Separation of the laminar boundary layer on the plate is caused by an adverse pressure gradient imposed by a curved wall opposite to the plate. The instability of, and transition process in, the separation bubble are focused on. The bubble is found to be highly susceptible to high-frequency two-dimensional instability waves, which are studied under both natural and forced conditions. A similar development of these instability waves in the separation bubble is found in both cases. The exponential growth of the two-dimensional disturbances dominates the flow except for in the reattachment region, where large-scale three-dimensional structures appear. Some difficulties associated with experimental investigations of boundary-layer separation-bubble flows are discussed.

Keywords: laminar separation bubbles; instability waves; laminar turbulent transition; reattachment

1. Introduction

This paper is concerned with the separation of a laminar boundary layer due to an adverse pressure gradient and the transition from laminar to turbulent flow. The laminar (transitional) separation bubble has previously been studied with different approaches—theoretical, numerical and experimental—which have given insight into this complex flow field, but a description of the transition process in the separation bubble is far from complete. In fact, experimental studies focusing on the transition process in adverse-pressure-gradient-induced laminar separation bubbles are scarce, despite the importance of this flow in many engineering applications. This can probably be explained partly by the difficulties with, and shortcomings of, the available measurement techniques for separated flows in general.

A schematic picture of the flow studied is given in figure 1, in which the wall-normal direction has been stretched for clarity. A low-velocity region, termed the separation bubble, is surrounded by a separated shear layer, which reattaches to the surface downstream of the bubble. Separation of the laminar boundary layer is caused by a retardation of the external flow due to an adverse pressure gradient. The point of separation and the forward portion of the bubble are steady compared with the highly unsteady flow in the vicinity of the reattachment point. The

† Present address: Volvo Car Cooperation, S-40531 Göteborg, Sweden.
‡ Present address: Chalmers University of Technology, Thermo and Fluid Dynamics, S-412 96 Göteborg, Sweden.

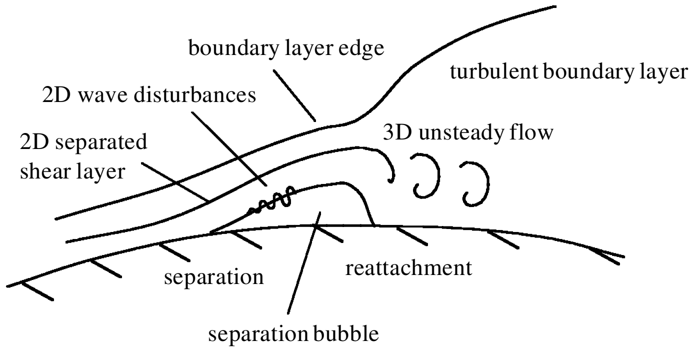

Figure 1. Laminar separation-bubble flow due to an adverse pressure gradient.

separation bubble depicted in figure 1 should be distinguished from the case where boundary-layer separation is caused by sharp gradients of the wall surface: geometry-induced separation. The differences in the physics of the flow between these two cases of separation are discussed by Alving & Fernholz (1996) and Dovgal *et al.* (1994).

In early experimental work on laminar separation bubbles, much effort was devoted to determining empirical correlations between global quantities of the bubble and boundary-layer properties at the point of separation, and devising semi-empirical theories for predicting what kind of bubble would occur in a given flow situation. A review is given by Tani (1964). The effect of laminar separation bubbles on the stalling characteristics of different aerofoils was also focused on (see Ward 1963).

Gaster (1966) investigated laminar separation bubbles on a flat plate caused by an adverse pressure gradient for a broad range of Reynolds numbers and pressure distributions. The pressure gradient was established by an aerofoil mounted above the flat plate. The aerofoil was equipped with a system for blowing through a slot at the surface in order to prevent stall. In contrast to the present investigation, where a curved wall with suction was employed to produce the adverse pressure gradient, this arrangement causes disturbances in the external stream, originating from the jet and the trailing-edge wake of the aerofoil, which can influence the separated region at the plate. Gaster (1966) found that the length of the separation bubble suddenly increased when the adverse pressure gradient and/or the Reynolds number exceeded certain critical values: so-called bubble bursting. Pauley *et al.* (1990) studied separation bubbles numerically by modelling Gaster's experiment and found that the bursting was due to periodic vortex shedding from the bubble, and that the longer bubble in Gaster's experiment was the result of time averaging of that shedding. Furthermore, Pauley *et al.* (1990) found that the shedding frequency agreed with the predicted most-amplified linear inviscid instability of the separated shear layer.

Recent experiments and direct numerical simulations have shown that instability and unsteadiness of laminar separation bubbles arise from the growth of low-amplitude instability waves in the boundary layer, a process which can start upstream of separation (Dovgal *et al.* 1994; Gruber *et al.* 1987; Rist & Maucher 1994; Hildings 1997).

2. Some difficulties associated with experiments on laminar separation bubbles

The experimentalist investigating laminar separation bubbles encounters several particular problems due to the complexity of separated flows. As a background we will briefly bring up some of these difficulties.

Hot-wire anemometry has been successfully used to give accurate and detailed measurements with high time resolution and space resolution in transition experiments featuring high-frequency disturbance waves with low amplitudes. However, conventional measurements using single hot-wire techniques in reverse-flow regions give erroneous results due to the insensitivity of the sensor element to the direction of the flow. In regions with reverse flow, the velocity signal will be folded, resulting, for instance, in a mean velocity that is too high. Nevertheless, using hot-wire techniques in laminar separation bubbles requires that the hot-wire probe be properly designed and of an appropriate size in order to avoid interference with the bubble. At the leading edge of a low-Reynolds number aerofoil, separation will take place downstream of the suction peak where the boundary layer is very thin. A typical size for a leading-edge bubble could be only a fraction of a millimetre in height and a couple of millimetres in length.

Another difficulty arises from the fact that the laminar separation bubble is highly sensitive to various kinds of perturbations in the flow: both disturbances in the external stream, such as mean flow variations, acoustic disturbances, freestream turbulence, etc.; and surface vibrations and roughness. This puts high demands on the quality of the 'natural', i.e. unforced, flow in wind-tunnel experiments in order to be able to isolate and quantitatively compare the effects of different types of artificially generated disturbances on the separated flow.

The laminar separation-bubble flow also shows an intrinsic unsteadiness. A small variation in inflow conditions can result in unsteadiness and a considerable movement of the separation point in the streamwise direction, but also in global changes of the flow in the form of stochastic oscillations between separated and non-separated flow. This can be caused by fluctuations in the adverse pressure gradient, which is usually applied by an auxiliary displacement body or suction slot. Even if the separation point is steady, the two dimensionality is sensitive to pressure gradients in the spanwise direction, which will cause the separation line to be curved.

In separated flows strong hysteresis effects can prevail, a complex phenomenon of which little is known. The structure of the separated flow then depends on the flow history, for instance initial variations in pressure gradient and Reynolds number at the start-up of the experiment.

Together these factors make it complicated to establish experimental conditions enabling accurate and reproducible measurements.

3. Experimental set-up and measurement technique

The measurements were carried out in the MTL wind tunnel at KTH, Stockholm. This wind tunnel is designed for transition experiments, providing a low freestream turbulence level ($Tu = 0.02\%$†) and acoustic noise level. In figure 2 a sketch of the

† The freestream turbulence level of the tunnel was determined with an empty test section at 25 m s^{-1}, for frequencies above 10 Hz, corresponding to scales smaller than 2.5 m (see Johansson 1992).

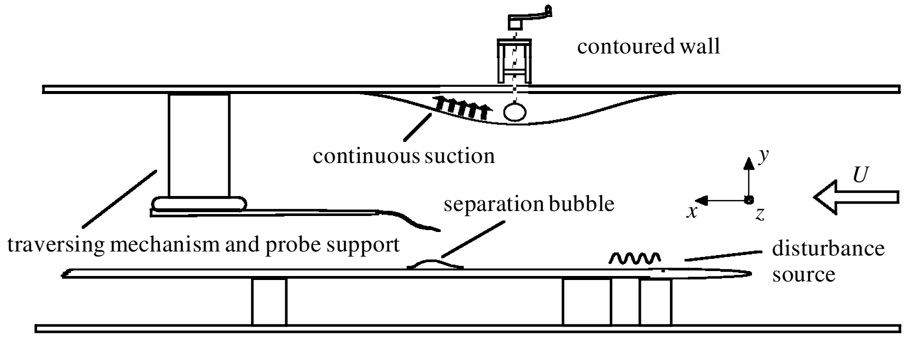

Figure 2. Experimental set-up in the MTL wind tunnel.

present test section set-up is shown. The height of the test section is 0.8 m and its width is 1.2 m.

In the test section, a flat plate with an asymmetric leading edge and a trailing-edge flap is installed. Further details about the wind tunnel and the flat plate can be found in Klingmann *et al.* (1993). An adverse pressure gradient is imposed on the laminar boundary layer on the plate by an adjustable contoured wall mounted in the test section. The contoured wall consisted of an aluminium rig in which a 1 mm thick aluminium sheet was attached at one end and free to slide at the other end. The shape of the inserted wall could be changed by manually displacing a threaded rod in the vertical direction. The end of this rod was connected to an iron bar, horizontally aligned and positioned perpendicular to the flow direction. This bar spanned the width of the test section and kept the aluminium sheet under tension and parallel to the flat plate.

In order to prevent separation at the curved wall, suction was applied through a $1.2 \times 0.3\ \mathrm{m}^2$ porous section of the aluminium sheet at the leeward side of the contraction. The fraction of the flow in the test section removed through the porous section was *ca.* 0.5–1.0%. By applying suction, the flow remained attached all along the curved wall.

The adverse pressure gradient, imposed by the contoured wall, causes the laminar boundary layer at the plate to separate. Reattachment of the unstable separated shear layer further downstream results in the formation of a laminar separation bubble with an average length and height of *ca.* 200 mm and *ca.* 3 mm, respectively. This fairly large size of the separation bubble made detailed measurements in the bubble with a hot wire possible.

The streamwise velocity component of the flow in the separation bubble was measured with a 2.5 μm platinum single hot wire, which could be traversed by a five-axis traversing system. Calibration was performed upstream of the contraction against a Pitot tube connected to a highly accurate pressure transducer. During calibration of the probe and during measurements the ambient air temperature in the wind tunnel was kept constant within ±0.1 °C by the cooling system of the wind tunnel.

A Cartesian coordinate system is adopted with its origin on the centreline at the leading edge of the plate. The velocity components in the streamwise, x, wall-normal, y, and spanwise, z, directions are denoted by u, v and w, respectively.

The boundary layer on the plate was traversed with the single hot wire, and time traces of the anemometer signal were recorded at each measurement point at a

PHILOSOPHICAL TRANSACTIONS OF THE ROYAL SOCIETY A MATHEMATICAL, PHYSICAL & ENGINEERING SCIENCES

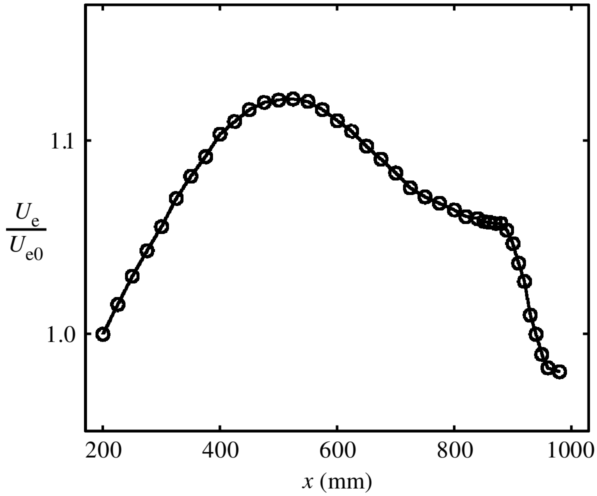

Figure 3. Streamwise variation of the edge velocity, U_e/U_{e0}.

sampling frequency of 2.0 kHz. The streamwise spacing, Δx, between two consecutive profiles was 25, 20 or 10 mm, with the denser spacing used in the latter part of the bubble. Δx = 10 mm corresponded to *ca.* 5% of the total length of the separation bubble and a typical series of measurements consisted of 30 vertical profiles, each containing 20–40 points depending on x.

Controlled disturbances could be generated in the boundary layer by suction and blowing at the wall through a 330×0.8 mm^2 slot in a flush-mounted plug in the plate. The slot is located at x = 189 mm, approximately three bubble lengths upstream of the point of separation, perpendicularly aligned to the direction of the flow. At the lower side of the plug 40 inlet pipes are mounted, connected by flexible hoses to loudspeakers. By feeding the loudspeakers with phase- and amplitude-controlled signals generated by a computer, different types of wave disturbances can be generated (see Elofsson 1998). The disturbance wave generation, the data acquisition and the traversing of the hot-wire probe were all fully computer controlled.

4. Results

(*a*) *Mean flow*

The variation of the edge velocity, U_e, i.e. the velocity in the outer inviscid flow, along the plate is shown in figure 3. U_e is normalized with a reference velocity at the leading edge, $U_e(x = 0) = U_{e0} = 7$ m s^{-1}, which was kept constant in these experiments. The laminar boundary layer on the plate is first accelerated, reaching a maximum velocity approximately at the throat of the contraction at $x \approx 550$ mm. Thereafter the flow is decelerated, followed by separation. Outside the separation bubble U_e becomes fairly constant, a region referred to in the literature as the 'pressure plateau', since the static pressure at the wall becomes constant there. Further downstream an abrupt decrease in U_e occurs, which is associated with reattachment. Here, the separation point does not coincide with the beginning of the 'pressure plateau', but is located further upstream.

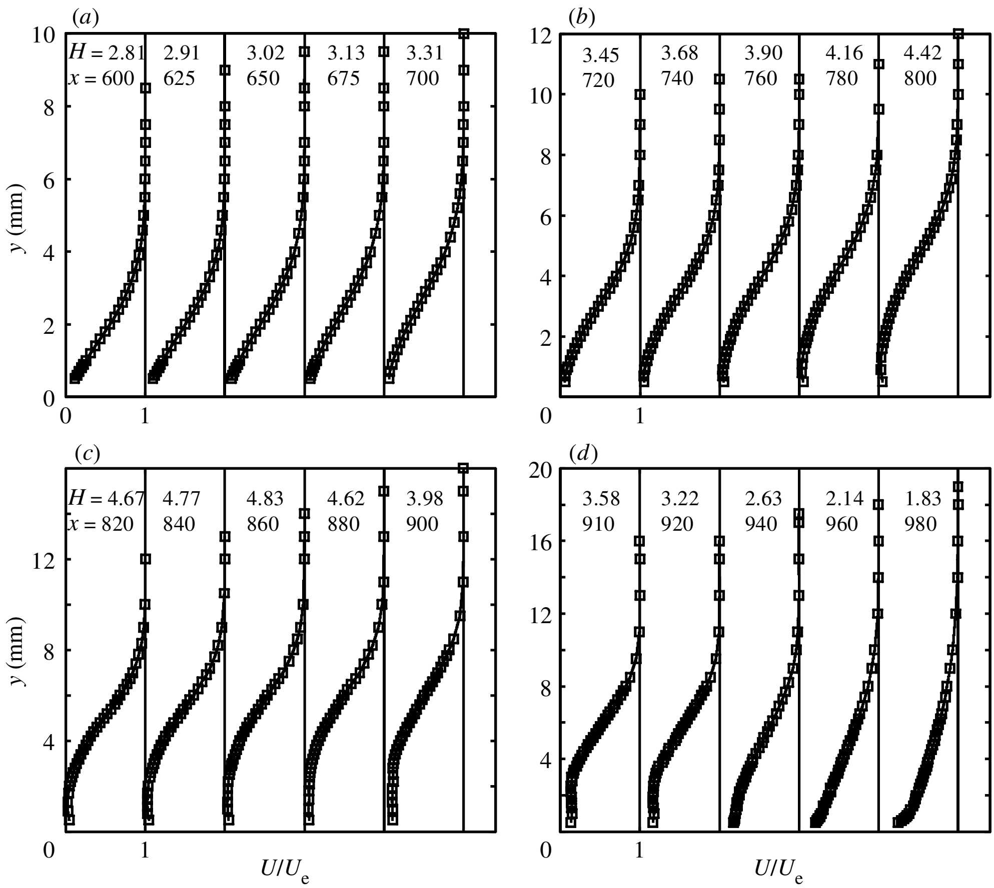

Figure 4. Mean velocity profiles along the plate centreline. Streamwise positions are given in millimetres from the leading edge.

Figure 4 shows profiles of the streamwise mean velocity component, normalized with the edge velocity, U_e, at several downstream positions. The actual separation bubble appears as the part of the velocity profile near the wall, where the velocity seems to be independent of y and not approaching zero. This is due to the inability of the single wire to detect the flow direction. Comparing, for example, the profiles at $x = 860$ mm and at $x = 900$ mm, the vertical extent of this constant velocity region is seen to increase downstream.

Due to the behaviour of the single wire in reverse-flow regions mentioned above, the hot-wire measurements could only give an approximate location of the separation and reattachment points. These were more accurately determined from smoke visualizations. Separation and reattachment were hereby found to occur at $x_s \approx 700$ mm and $x_r \approx 900$ mm, respectively. The Reynolds number based on U_{e0} and the distance from the leading edge to the point of separation, x_s, was $Re_x = U_{e0}x_s/\nu = 3.3 \times 10^5$.

The variation with x of the integral flow parameters—i.e. the displacement thickness δ^*, the momentum loss thickness θ and shape factor, $H = \delta^*/\theta$—is illustrated in figure 5. The Reynolds numbers based on the edge velocity at separation, U_s, and the displacement thickness, δ^*_s or momentum thickness at separation, θ_s, were

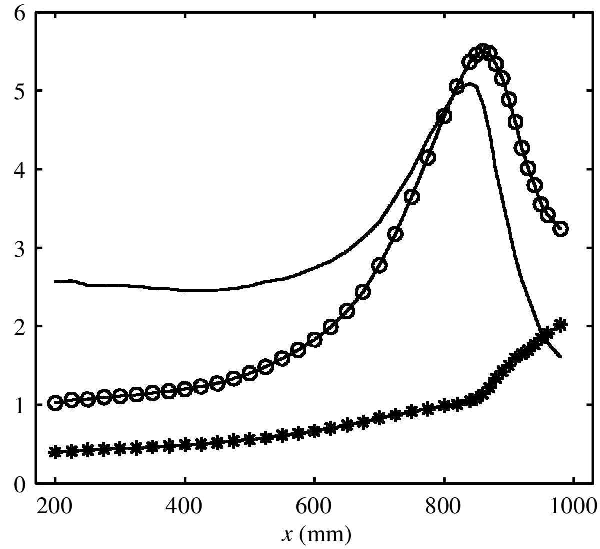

Figure 5. Integral flow parameters: –o–o–, δ^* (mm); –∗–∗–, θ (mm); ——, H.

$Re_{\delta^*_s} = 1390$ and $Re_{\theta_s} = 417$, respectively. Inside the region of the bubble, θ remains fairly constant in comparison with δ^*. Not until $x \approx 870$ mm does θ increase as the unstable separated shear layer reattaches and a turbulent boundary layer develops. δ^* on the other hand shows an enhanced growth upstream of the separation point, reaching a maximum value at $x = 860$ mm, and from there on decays as the mean velocity profile gets fuller. The shape factor reaches a maximum value of approximately 5 in the separation bubble. Since no backflow is measured in the reverse-flow region in the bubble, δ^* will be underestimated and θ overestimated in the numerical integrations of the mean velocity profiles in the bubble. The values in figure 5 should therefore be considered as indicative, and should not be used for determining the points of separation and reattachment.

(*b*) *Natural velocity fluctuations*

The natural, i.e. unforced, laminar separation-bubble flow in the present investigation is highly unstable. Initially disturbances in the boundary layer are damped in the favourable-pressure-gradient region upstream of the bubble, but further downstream the rapid disturbance growth in the adverse-pressure-gradient boundary layer and in the separated shear layer causes transition and a turbulent boundary layer is established after reattachment.

Figure 6 shows amplitude spectra of the streamwise velocity inside the separated shear layer at $x = 830$, 840 and 850 mm. The dominating natural velocity fluctuations in the separated shear layer in the bubble have disparate time-scales. The natural fluctuations can broadly be divided into low-frequency oscillations (here frequencies less than 20 Hz) and high-frequency oscillations (in this case frequencies in the range 60–120 Hz). The presence of low-frequency fluctuations in the separation bubble is a characteristic feature of separated flows in general, and is not restricted to the case where separation is caused by an adverse pressure gradient (Cherry *et al*. 1984). The origin of this low-frequency motion is not fully clear but may be due to a global

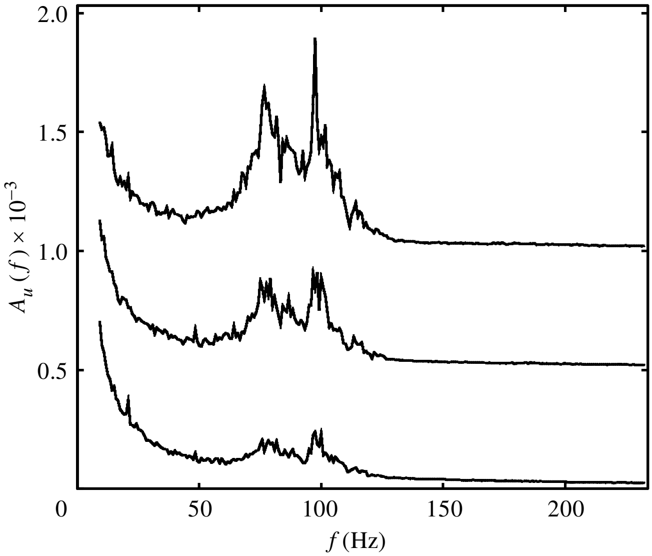

Figure 6. Amplitude spectra of streamwise velocity, $A_u(f)$, in the separated shear layer at $x = 830$, 840 and 850 mm and $y = 5.2$ mm under natural conditions. The spectra are shifted in amplitude by a factor of 0.5×10^{-3} for clarity.

instability, which is especially manifested in the reattachment region and gives rise to an overall 'flapping' motion of the separated shear layer, observed by Dovgal *et al.* (1994) among others. The high-frequency fluctuations in figure 6 are seen to increase downstream, which illustrates that naturally occurring disturbances within this frequency range grow rapidly.

(*c*) *Artificially forced instability waves*

The development of low-amplitude two-dimensional instability waves in the separation bubble was investigated further by means of controlled generation by suction and blowing through the transverse slot in the plate located at $x = 189$ mm. When using artificial excitation a phase reference exists, and the downstream development of the phase of the instability wave can be measured with one probe. The frequency of the forced instability wave was chosen to agree with one of the most amplified frequencies in the natural bubble, $f^* = 83.3$ Hz.

Close to the disturbance source the instability wave resembles a Tollmien–Schlichting wave in the Blasius boundary layer with two local maxima in the amplitude distribution of the fluctuating streamwise velocity. When entering the separated region, the amplitude distribution of the instability wave changes shape and develops a third local maximum in the shear layer. Similar behaviour was observed for the naturally excited high-frequency waves prior to reattachment. Figure 7 compares the wall-normal distribution of the amplitude of the forced wave at three streamwise positions close to reattachment with a filtered RMS distribution of the fluctuating streamwise velocity in the natural case, where the time signals were bandpass filtered in the range 40–133 Hz. The corresponding mean velocity profiles are plotted in the same graphs. The three maxima are, both in the natural case and in the forced case,

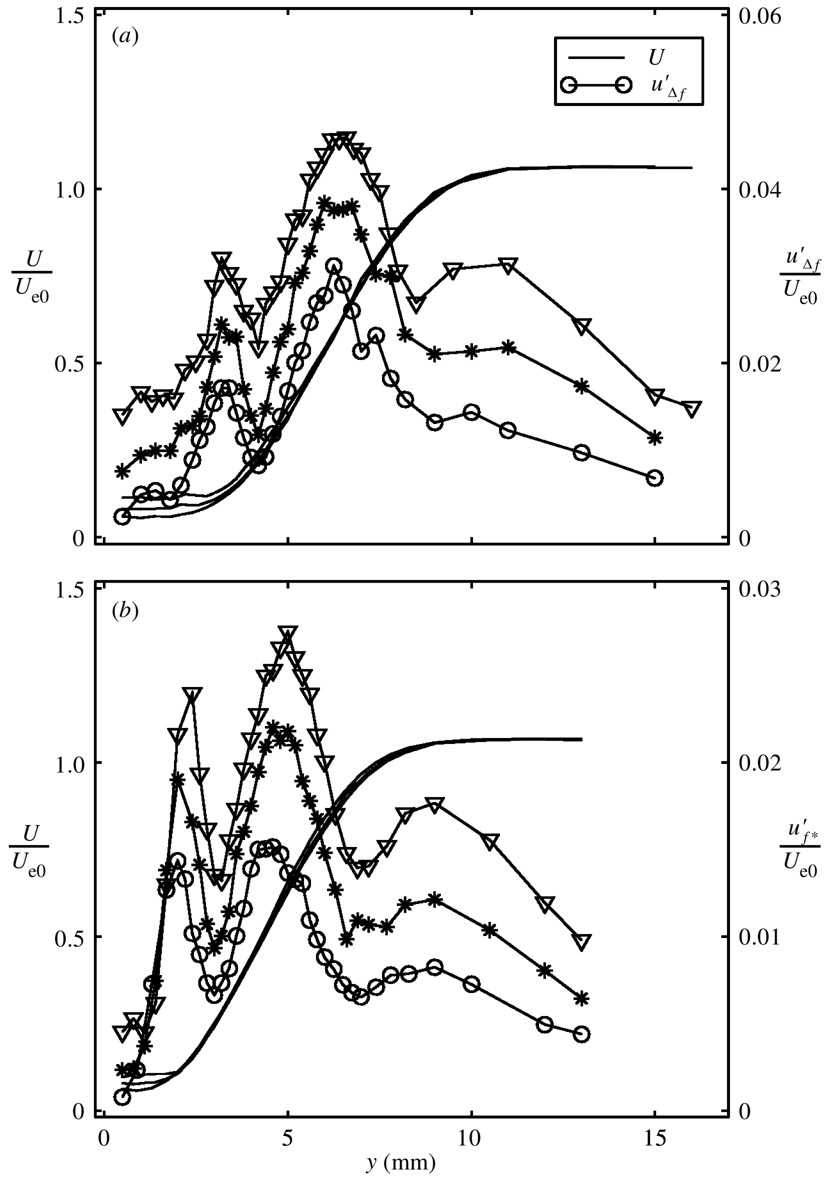

Figure 7. Amplitude profiles of natural and forced instability waves prior to reattachment. Measurements at $x = 880$ (–o–o–), 890 (–∗–∗–) and 900 mm (–▽–▽–) in the natural flow case (*a*), and at $x = 830$ (–o–o–), 840 (–∗–∗–) and 850 mm (–▽–▽–) in the forced case (*b*).

located at the edge of the low-velocity region, at the inflection point of the separated shear layer, and at its edge, respectively.

Figure 8 shows the wall-normal phase profile of the forced instability wave at $x = 840$ mm (*b*) together with the streamwise phase variation of the middle amplitude maximum of the wave (*a*). Two phase shifts exist in the phase profile at $x = 840$ mm, located between regions of constant phase, which correspond to the three local amplitude maxima seen in figure 7. From the downstream phase development of the middle

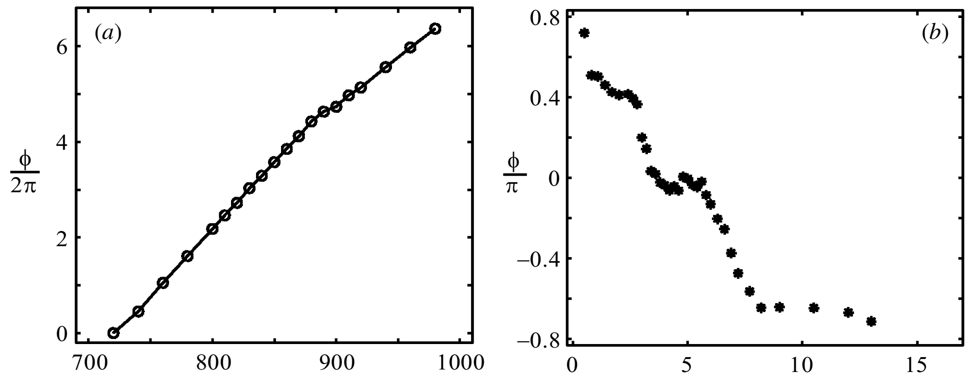

Figure 8. Phase development (the phase is determined at the middle maxima) in the streamwise direction (*a*) and wall-normal phase profile at $x = 840$ mm (*b*) of the two-dimensional instability wave in the separation bubble. The frequency is 83.3 Hz.

amplitude maximum, the phase speed, c, of the instability waves can be determined as

$$c = \omega \bigg/ \frac{\Delta\phi}{\Delta x},$$

where $\omega = 2\pi f^*$. c is found to be nearly constant in the region where the separation bubble is located until reattachment occurs. At $x = 840$ mm, $c/U_e = 0.39$. This is lower than the mean velocity at the inflection point at the same streamwise position, which equals $0.60U_e$. One may have expected that the phase speed of the waves would be closer to the mean velocity at the inflection point as would be the case in a free shear layer flow, but, as Michalke (1990) has shown, the influence of the wall reduces the wave speed quite significantly for wavelengths that are larger than the distance of the inflection point from the wall. In fact, our measured phase speed is close to values corresponding to his numerical results.

The streamwise growth of the forced two-dimensional wave is shown in figure 9. The instability wave grows exponentially between $x \approx 700$ and $x \approx 825$ mm and saturates after reattachment at an amplitude above 10%. This growth starts upstream of separation, in the adverse pressure gradient boundary layer, where a factor 5 increase in amplitude is observed from $x \approx 600$ to $x_s \approx 700$ mm.

The disturbance growth in the bubble is quite high; the separation bubble has the ability to amplify the wave by almost three orders of magnitude in a streamwise distance of 200 mm, corresponding to approximately five wavelengths.

(*d*) *Flow visualizations*

The flow in the separation bubble was visualized by introducing a thin layer of smoke through a narrow slot in the plate 212 mm downstream of the leading edge. A photograph of the flow in the case of natural transition is shown in figure 10. The flow is from left to right and the scale in the upper part of the photograph is in mm, with zero at the leading edge. In the laminar boundary layer ahead of the bubble, the smoke sheet is smooth and unperturbed. The separation line can be seen around $x = 700$ mm. The bubble remains fairly two dimensional and steady from the point of separation up to $x \approx 860$ mm. Before the reattachment region two wave

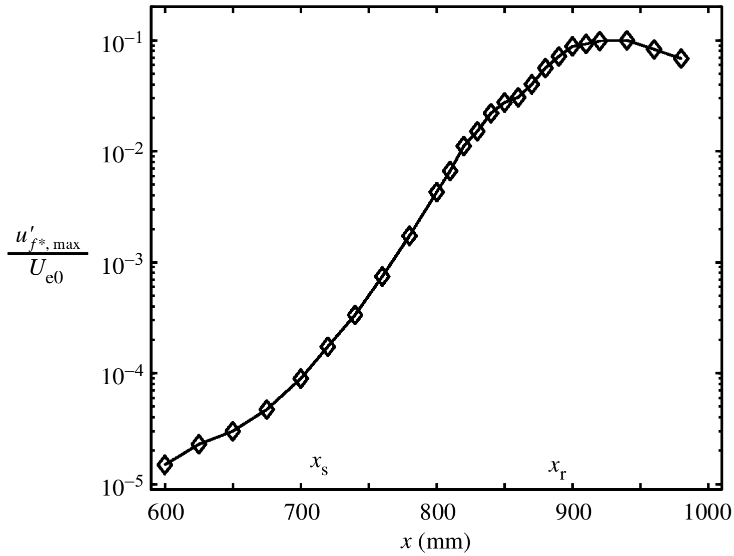

Figure 9. Amplification curve of forced two-dimensional instability wave in the separation bubble with $f^* = 83.3$ Hz.

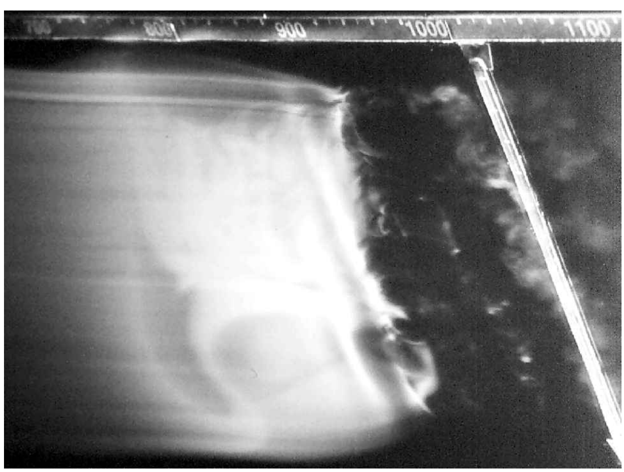

Figure 10. Instantaneous smoke visualization of the separation bubble under natural conditions.

crests can be distinguished, whereafter the smoke sheet is dispersed, although a weak three-dimensional structure is visible.

In figure 11 the flow is forced through the slot at x =189 mm with a frequency of 102 Hz. For this case several waves can be seen, which are initially highly two dimensional. The breakup occurs at almost constant x across the full span of the smoke sheet, and here a three-dimensional streamwise oriented pattern is clearly seen in and after the reattachment region. From video recordings it was observed that the three-dimensional structure was fairly steady in the spanwise direction and had a spanwise wavelength of *ca.* 30 mm.

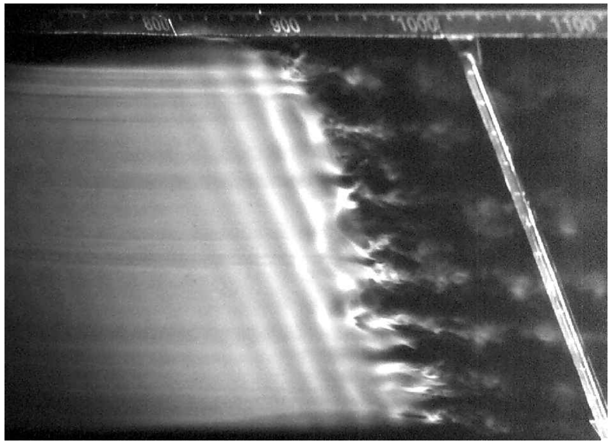

Figure 11. Instantaneous smoke visualization of the separation bubble when forcing a two-dimensional instability wave. $U_{e0} = 5.0\ \mathrm{m\ s^{-1}}$ and the forcing frequency is 102 Hz.

5. Summary and conclusions

A two-dimensional laminar separation bubble induced by an adverse-pressure gradient was studied experimentally in a wind tunnel. The set-up employed a contoured wall with boundary-layer suction to induce the pressure gradient and resulted in a bubble with a stable, two-dimensional separation line. The present experiments combine flow visualization, hot-wire measurements and an accurate wave disturbance forcing technique to make detailed measurements of the evolution of single-frequency two-dimensional instability waves in the separating and reattaching boundary layer, as well as naturally occurring wave disturbances.

The present investigation is in qualitative agreement with previous studies on laminar separation, but is unique in its set-up and level of detailed measurements. Several new interesting aspects of disturbance growth were also observed. We summarize the main results below.

(1) The streamwise velocity disturbance distribution for both natural and forced disturbances shows three maxima. The largest amplitude corresponds to the inflection point in the mean velocity, indicating an inviscid origin of the disturbance.

(2) The phase speed of the disturbance is lower than the velocity at the inflection point. This is probably an effect of the wall, which has theoretically been shown to lower the phase speed as compared with a free shear layer (Michalke 1990).

(3) The growth rate of wave disturbances in the bubble was found to be exponential, and the wave amplitude of the forced wave reaches a value of *ca.* 10% of the edge velocity before it saturates. These results are in excellent agreement with theoretical results by Hildings (1997) (both direct numerical simulation and linear stability calculations), where the base flow was obtained from the present experiments.

(4) The flow visualization shows the formation of three-dimensional well-ordered structures before reattachment. These structures have a spanwise wavelength that is about the same as the wavelength of the two-dimensional wave.

PHILOSOPHICAL TRANSACTIONS OF THE ROYAL SOCIETY A MATHEMATICAL, PHYSICAL & ENGINEERING SCIENCES

This work was supported by the Swedish Research Council for the Engineering Sciences (TFR). The stay of A.A.B. at KTH was financed through a Göran Gustafsson Foundation post-doctoral position. The flow visualizations were carried out in cooperation with Dr Matsubara. Dr Elofsson is acknowledged for providing the wave-disturbance generator.

References

Alving, E. & Fernholz, H. H. 1996 Turbulence measurements around a mild separation bubble and downstream of reattachment. *J. Fluid Mech.* **322**, 297–328.

Cherry, N. J., Hillier, R. & Latour, M. E. M. P. 1984 Unsteady measurements in a separated and reattaching flow *J. Fluid Mech.* **144**, 13–46.

Dovgal, A. V., Kozlov, V. V. & Michalke, A. 1994 Laminar boundary layer separation: instability and associated phenomena. *Prog. Aerospace Sci.* **30**, 61–94.

Elofsson, P. 1998 Experiments on oblique transition in wall bounded shear flows. PhD thesis, TRITA-MEK Technical Report 1998:5, Department of Mechanics, KTH.

Gaster, M. 1966 The structure and behaviour of laminar separation bubbles. In *Proc. Conf. AGARD, Rhode-Saint-Genese, Belgium, 10–13 May 1966*, paper no. 4, pp. 813–854.

Gruber, K., Bestek, H. & Fasel, H. 1987 Interaction between a Tollmien–Schlichting wave and a laminar separation bubble. AIAA Paper 87-1256.

Hildings, C. 1997 Simulation of laminar and transitional separation bubbles. TRITA-MEK technical report 1997:19, Department of Mechanics, KTH.

Johansson, A. V. 1992 A low speed wind-tunnel with extreme flow quality—design and tests. In *Proc. 18th ICAS Congress, Beijing, September 1992*, pp. 1603–1611.

Klingmann, B. G. B., Boiko, A. V., Westin, K. J. A., Kozlov, V. V. & Alfredsson, P. H. 1993 Experiments on the stability of Tollmien–Schlichting waves. *Eur. J. Mech.* B **12**, 493–514.

Michalke, A. 1990 On the inviscid instability of wall-bounded velocity profiles close to separation. *Z. Flugwiss. Weltraumforsch.* **14**, 24–31.

Pauley, L. L., Moin, P. & Reynolds, W. C. 1990 The structure of two-dimensional separation. *J. Fluid Mech.* **220**, 397–411.

Rist, U. & Maucher, U. 1994 Direct numerical simulation of 2-D and 3-D instability waves in a laminar separation bubble. In *Proc. Conf. Application of Direct and Large Eddy Simulation to Transition and Turbulence, AGARD CP-551, Chania, Crete, April 18–21*, pp. 34.1–34.7.

Tani, I. 1964 Low-speed flows involving bubble separations. *Prog. Aerospace Sci.* **5**, 70–103.

Ward, J. W. 1963 The behaviour and effects of laminar separation bubbles on aerofoils in incompressible flow. *J. R. Aero. Soc.* **67**, 783–790.